Eur. Phys. J. D **9**, 179–182 (1999)

THE EUROPEAN PHYSICAL JOURNAL D

EDP Sciences

Ionization potential of Al_6 and Al_7 as a function of temperature

J. Akola[1], H. Häkkinen[2], and M. Manninen[1]

[1] Department of Physics, University of Jyväskylä, P.O. Box 35, FIN-40351 Jyväskylä, Finland
[2] School of Physics, Georgia Institute of Technology, Atlanta, GA 30332-0430, USA

Received: 1 September 1998 / Received in final form: 5 October 1998

Abstract. The temperature-depence of the ionization potential of Al_6 and Al_7 clusters is studied by using *ab initio* molecular dynamics. The threshold regions of theoretical photoionization efficiency curves are obtained from the calculated ionization potential distributions by integration and the determined ionization potentials are compared with the experimental ones. Two important effects, which complicate the determination of ionization potential from photoionization efficiency curves, are observed: the thermal tail effect and the isomerization. Also a link between the adiabatic ionization potential and the threshold of the photoionization efficiency curve is discussed. In the case of Al_7, this often used connection breaks down.

PACS. 36.40.Cg Electronic and magnetic properties of clusters – 36.40.Mr Spectroscopy and geometrical structure of clusters – 71.24.+q Electronic structures of clusters and nanoparticles

1 Introduction

Although the concept of ionization potential (IP) is a very simple one, interpretation of the experimental ionization potential of clusters has been difficult due to thermal and quantum mechanical effects. These effects are related to the experimental setup, where there is always a finite temperature, and to the ionization process itself, which involves an incoming photon and an outgoing photoelectron. As a result thermal tails and local maxima are observed in photoionization efficiency (PIE) spectra. The problem now is to interpret these features and to extract ionization potential (vertical or adiabatic) out of the spectra.

There are still only a few theoretical studies concerning photoionization process of clusters. Photoionization cross sections have been calculated for small alkali clusters by using both jellium [1] and *ab initio* models [2]. In addition temperature-dependent cross sections for alkali clusters [1] and direct temperature-dependent ionization potentials for K and Ag clusters [3] have been calculated by using ellipsoidal jellium model.

In this paper we present a straightforward way to study theoretically the threshold regions of PIE curves as a function of temperature. The PIE curves are obtained from the IP distributions of Al_6 and Al_7 clusters during an *ab initio* molecular dynamics and the determined ionization potentials are compared with the experimental ones [4, 5]. We want to emphasize here that we are only interested in PIE curves near the threshold, which justifies our neglect of high energy phenomena such as innercore ionization and photoinduced fragmentation. We will also neglect the plasmon effects which are expected to be small for small clusters [1].

2 Method

The calculations are done using the BO–LSD–MD (Born–Oppenheimer local-spin-density molecular dynamics) method devised by Barnett and Landman, fully documented in [6]. The ions move according to classical molecular dynamics in the force field calculated in each time step using the LSD approximation and pseudopotentials [7]. We use a plane wave basis but we wish to stress that the method does not apply any of the standard supercell techniques in calculating the total energy of a finite system. This is an important aspect pertinent to this study: the ionization potential can be calculated as a straightforward difference in the total energies of the neutral and charged cluster, without or with the relaxation of the charged cluster to evaluate the vertical (vIP) or adiabatic (aIP) ionization potential, respectively.

We use an MD run, where all coordinates and Kohn–Sahm (KS) state energies are recorded for every time step of 5 fs, as a starting point of our study. Instead of calculating the IP's from this data as total energy differences between neutral cluster and ion, we use an alternative method which is based on Slater's transition state approach [8] and Janak's theorem for density functional theory [9, 10]

$$\frac{\partial E}{\partial n_i} = \varepsilon_i \,, \tag{1}$$

where E is the total energy of the system, n_i and ε_i are the occupation number and the energy of the highest occupied KS state (so called HOMO state), respectively. An immediate consequence of this theorem is that

$$I = E_{N-1} - E_N = -\int_0^1 \varepsilon_i(n)\mathrm{d}n \tag{2}$$

where I is the ionization potential and N is the total number of electrons in a neutral cluster. We studied the above presentation (2) of IP for the ground states of Al_6 and Al_7 and it holds perfectly for both of these clusters. We also noticed that ε_i is practically a linear function of n_i and that with a high accuracy

$$I \approx -\varepsilon_i(0.5)\,. \tag{3}$$

By using these facts we can make an assumption that

$$I \approx -\varepsilon_i(1.0) + c\,, \tag{4}$$

where c is a constant. In order to check out the validity of this assumption for Al_6 and Al_7, respectively, we explicitly calculated the ionization potentials and the constants c for 30 configurations, which were randomly chosen from MD runs at 600–800 K. From the resulting distributions we observed that while the deviations of IP were about 0.6–0.8 eV, the values of c were within 0.1 eV. This allows us to estimate the IP from the energy eigenvalues of the highest occupied KS states. We can first plot a time-averaged distribution of the HOMO level values by replacing the level of each time step by a narrow gaussian. By shifting this KS energy level distribution by the constant c we finally get the IP distribution which corresponds to the derivative of the PIE curve in our simplified model, where we assume the transition matrix element to be a constant.

In order to compare our results with experiments, we will use the same methods for the IP determinination as experimentalists. Near the threshold region of the PIE curve we use two methods: the baseline intercept method, where one extrapolates the first linear rise to the baseline [11], and the pseudo-Watanabe method [12], where one seeks the first break from exponential behaviour. These two methods are often considered to produce the aIP. Beyond the threshold region we use a third method called error function fit [13–15]. This method seeks the first maximum of the derivative of PIE curve, and is considered to correspond to the vIP.

3 Results

The maximum temperature for all the MD runs was about 800 K. In the case of Al_6 we were able to see two dominant isomers below 600 K which coexisted even at the temperature of 100 K. Al_7 did not show this kind of thermal behaviour. The ground states of Al_6 and Al_7 and the isomer of Al_6 are shown in Fig. 1. Clearly we can see that both of the ground states have an octahedral origin. In addition we can see that the Al_6 isomer and the Al_7 ground state have common features. Thus the ground state of Al_7 resembles both of the Al_6 clusters. The obtained ground states and their IP's at 0 K (see Fig. 3) are in a good agreement with the results of Jones [16].

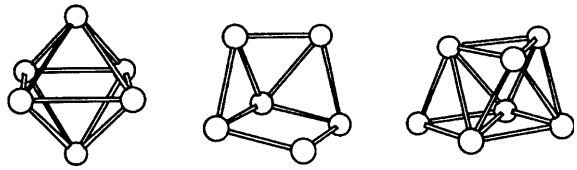

Fig. 1. Al_6 and Al_7 clusters. From left to right: Al_6 ground state, isomer and Al_7 ground state.

In Fig. 2 we present the KS energy distributions (absolute value) and the corresponding PIE curves for Al_6 and Al_7 at different temperatures. At 800 K Al_6 moves fast between the ground state and the isomer geometries. At lower temperatures transitions between isomers are too slow to be simulated. In Fig. 2 we show results at 300 K and 550 K only for MD of Al_6 isomer. The threshold behaviour of the IP is most likely determined by the isomer, since its IP is lower than that of the ground state. The differences between the KS energy distributions of Al_6 and Al_7 are obvious: the distributions of Al_7 are remarkably wider and the mean values of the distributions differ more than 0.2 eV. Another difference is that the upper boundary of the distribution of Al_7 moves to higher energy when the temperature is increased while the distribution of Al_6 seems to have a fixed upper boundary, which corresponds to the KS energy of the ground state. We should note that the oscillations of the distributions have a purely statistical origin due to the shortness of our MD runs. The width of the distribution for both clusters is proportional to $T^{1/2}$ as expected from the nearly harmonic motion of the ions.

The PIE curves of Al_7 have long thermal tails, which are understandable in terms of the jellium model, where 20 valence electrons correspond to a full electron shell and there is only one electron in the uppermost shell. This is fully consistent with the experimental PIE curves of small alkali metal clusters at a finite temperature [11, 12]. Because our PIE curves at 100 K show very short thermal tails for both Al_6 and Al_7, we can conclude that one can dampen the thermal tail effect by lowering the temperature below 100 K.

The ionization potentials were extracted from the PIE curves by using the three methods described above. These results are drawn in Fig. 3, where the two lower values correspond to the threshold region (aIP) and the upper ones correspond to the first maxima of the IP curve (vIP). The two aIP values are obtained by using pseudo-Watanabe and baseline intercept methods, respectively. The vIP values are obtained by fitting a gaussian to the IP distribution. The IP values at 0 K are the real vIP and aIP values of the Al_6 isomer and the Al_7 ground state. It is clearly seen that the trend of aIP is decreasing as a fuction of temperature. Also the thermal tail effect is visible as a large deviation of aIP values at higher temperatures. The vIP of Al_6 has similar decreasing behaviour as aIP's while the vIP of Al_7 does not differ much from the 0 K values. The little dip of the vIP of Al_6 at 600 K is due to isomerization effect as explained above. We want to point out especially

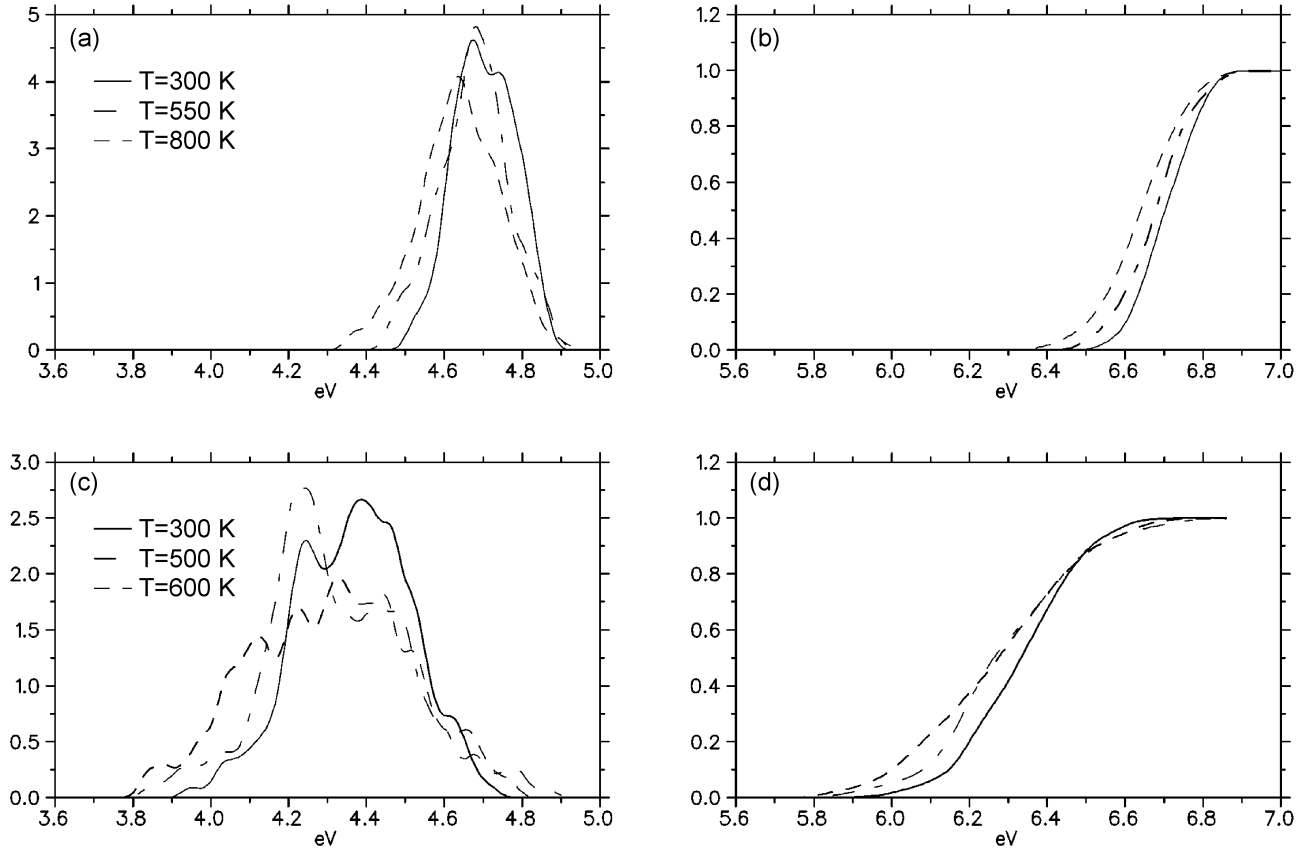

Fig. 2. KS energy absolute value distributions and corresponding PIE curves at different temperatures. (a) KS energy distribution and (b) PIE curve of Al_6; (c) KS energy distribution and (d) PIE curve of Al_7.

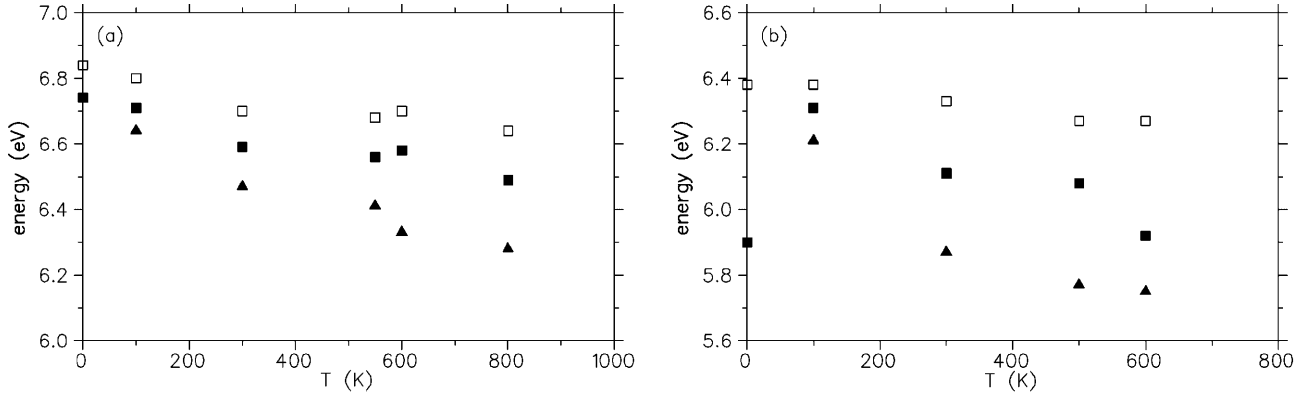

Fig. 3. Determined IP values of (a) Al_6 and (b) Al_7 at different temperatures. Open squares corresponding to vIP are obtained with error function fit and filled squares and triangles corresponding to aIP are obtained with baseline intercept and pseudo-Watanabe method, respectively.

that also the aIP curves extrapolate to the vIP at zero temperature, since the relaxation is not included. The true adiabatic value at $T = 0$ in the figure includes the ionic relaxation.

Next we compare our results with the experimental results [4, 5], which are obtained by using the bracketing method. In these experiments the temperature was near the room temperature. The experimental value of Al_6 is 6.45 eV, which is practically the same as we obtained with the pseudo-Watanabe method at 300 K. On the other hand the experimental IP value for Al_7 is 6.20 ± 0.20 eV while our value for aIP is 5.9 or 6.1 eV at 300 K. It is important to notice that the theoretical as well as the experimental value of the IP depends sensitively on the method used to determine it from the PIE curve.

Finally, we present in Fig. 4 the time-evolution of KS energies and the time-averaged distributions of the 18th and 21st KS single-particle states of Al_6 isomer and Al_7

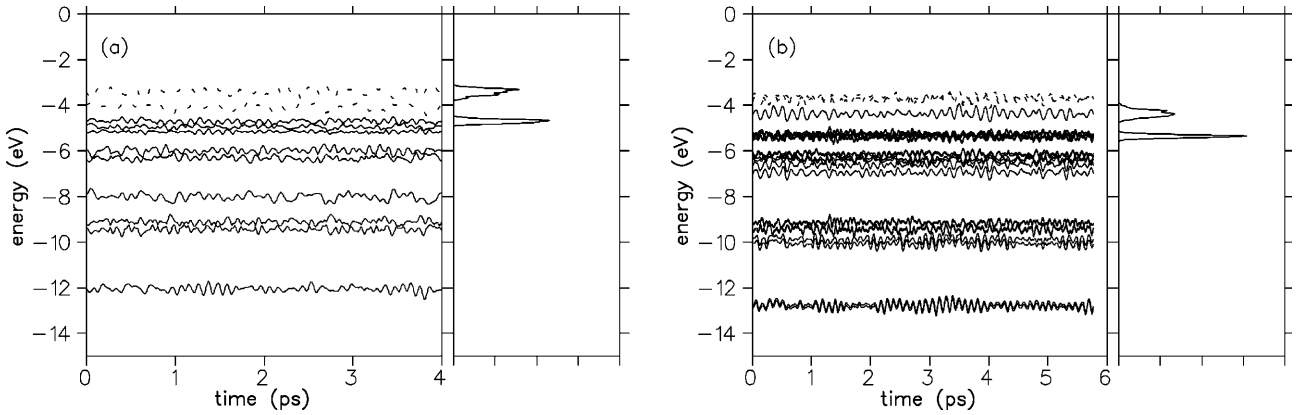

Fig. 4. Time-evolution of the KS energies and the time-averaged distributions of the 18th and 21st KS states of (a) Al_6 isomer and (b) Al_7 ground state at 300 K.

ground state at 300 K. For clarity the unoccupied KS states are drawn with dashed lines. We can see that our neglect of lower lying KS states in PIE curve determination is justified in both cases due to clear energy differences between the HOMO state and the lower KS states. The large energy gap between the highest and second highest KS state in Al_7 is in accordance with a jellium picture and explains the observed thermal tail effect of Al_7. Because of the geometrical similarities between Al_6 isomer and Al_7 ground state, common features in electronic structure can be seen. We see these especially from the time-averaged densities of KS states, where the disribution of 21st KS state is remarkably wider for both of these clusters.

4 Conclusion

In this paper we studied the temperature-dependence of the ionization potential of Al_6 and Al_7 clusters. The ground state electronic structures of these clusters are found to obey the jellium model. Al_6 has almost full outer valence electron shell while Al_7 has only one electron in its outer valence electron shell. During MD runs this electron seems to be particularly sensitive to the thermal motion of ions. As a result long thermal tails are seen in the calculated PIE curves of Al_7 at higher temperatures which is consistent to the experimental PIE curves of small alkali metal clusters [11, 12]. Theoretically determined ionization potentials are in good agreement with experimental results [4, 5]. This confirms the applicability of our simple method.

Al_6 was observed to have two coexisting isomers under 600 K. As pointed out in our earlier paper [17] this isomerization has to be taken into account, when determining the PIE curve for Al_6. As a result our IP values were more consistent with the experiments.

Usually one considers the threshold value of the PIE curve as the aIP. The success of this method relies on the fact that the aIP is usually near the threshold. We were able to show with Al_7, how this connection breaks down. This is because of the strong relaxation of the Al_7^+ cluster which transfers the aIP far below from the threshold value at 100 K. Therefore we conclude that one should be cautious, when interpreting an experimental PIE curve of small metal clusters. On the other hand we observe that the error function fit [14, 15] gives very good values for vIP at low temperatures (within 0.05 eV under 100 K). We recommend experimentalists to use this method, because comparisons to the calculations are easier to make. Unfortunately this kind of experimental data is not yet available for small metal clusters.

References

1. M. Koskinen, M. Manninen: Phys. Rev. B **54**, 14 796 (1996)
2. B. Wästberg, A. Rosen: Z. Phys. D **18**, 267 (1991)
3. C. Yannouleas, U. Landman: Phys. Rev. Lett. **78**, 1424 (1997)
4. D.M. Cox, D.J. Trevor, R.L. Whetten, A. Kaldor: J. Phys. Chem. **92**, 421 (1988)
5. K.E. Schriver, J.L. Persson, E.C. Honea, R.L. Whetten: Phys. Rev. Lett. **64**, 2539 (1990)
6. R.N. Barnett, U. Landman: Phys. Rev. B **48**, 2081 (1993)
7. N. Troullier, J.L. Martins: Phys. Rev. B **43**, 1993 (1991)
8. J.C. Slater: Adv. Quantum Chem. **6**, 1 (1972)
9. J.F. Janak: Phys. Rev. B **18**, 7165 (1978)
10. R.G. Parr, W. Yang: *Density-Functional Theory of Atoms and Molecules* (Oxford Science Publications, New York 1989)
11. W.A. Saunders, K. Clemenger, W.A. de Heer, W.D. Knight: Phys. Rev. B **32**, 1366 (1985)
12. M. Kappes, M. Schär, U. Röthlisberger, C. Yeretzian, E. Schumacher: Chem. Phys. Lett. **143**, 251 (1988)
13. H. Göhlich, T. Lange, T. Bergmann, U. Näher, T.P. Martin: Chem. Phys. Lett. **187**, 67 (1991)
14. H.G. Limberger, T.P. Martin: J. Chem. Phys. **90**, 2979 (1989)
15. T. Bergmann, T.P. Martin: J. Chem. Phys. **90**, 2848 (1989)
16. R.O. Jones: J. Chem. Phys. **99**, 1194 (1993)
17. J. Akola, H. Häkkinen, M. Manninen: Phys. Rev. B **58**, 3601 (1998)